

# An Efficient Multi-Domain Framework for Image-to-Image Translation

Ye Lin <sup>a</sup>, Keren Fu<sup>b</sup>, Shenggui Ling<sup>a</sup> and Cheng Peng <sup>\*c</sup>

<sup>a</sup>*National Key Laboratory of Fundamental Science on Synthetic Vision, Sichuan University, Chengdu, Sichuan 610065, China*

<sup>b</sup>*College of Computer Science, Sichuan University, Chengdu, Sichuan 610065, China*

<sup>c</sup>*School of Aeronautics and Astronautics, Sichuan University, Chengdu, Sichuan 610065, China*

## Abstract

Existing approaches have been proposed to tackle unsupervised image-to-image translation in recent years. However, they mainly focus on one-to-one mappings, making it difficult to handle more general and practical problems such as multi-domain translations. To address issues like large cost of training time and resources in translation between any number of domains, we propose a general framework called multi-domain translator (MDT), which is extended from bi-directional image-to-image translation. MDT is designed to have only one domain-shared encoder for the consideration of efficiency, together with several domain-specified decoders to transform an image into multiple domains without knowing the input domain label. Moreover, we propose to employ two constraints, namely reconstruction loss and identity loss to further improve the generation. Experiments are conducted on different databases for several multi-domain translation tasks. Both qualitative and quantitative results demonstrate the effectiveness and efficiency performed by the proposed MDT against the state-of-the-art models.

## 1 INTRODUCTION

In image processing, image-to-image translation is regarded as a mapping issue between two different image domains, which enables the input image to obtain features of another desired domain [1]. Many computer vision applications can be described as such, e.g., image segmentation [2], style transfer [3], image colorization [4], face synthesis [5] [6], image inpainting [7] [8] and super-resolution [9]. Traditionally, these tasks are tackled with specially designed machines [10] [11] [12], which attract many recent studies [1] [13] [14] [15] [16] [17] [18] to turn their attention to generally-purposed approaches. These state-of-the-art methods are mostly based on generative adversarial networks (GANs) [19], with the advantages of easy training, good visual quality and end-to-end applications of different scenarios in image processing.

These deep models usually use two kinds of settings, namely supervised and unsupervised, to learn mappings between different domains. The supervised ones [1] [13] need to train with paired data or the corresponding labels in target domain. However, it may be impractical or even impossible to acquire a large number of image pairs, making it difficult for more general and practical problems of image translation. By contrast, without needing paired images, the unsupervised ones [14] [15] are more applicable, since data preparation only involves splitting the data into

---

\*Corresponding author

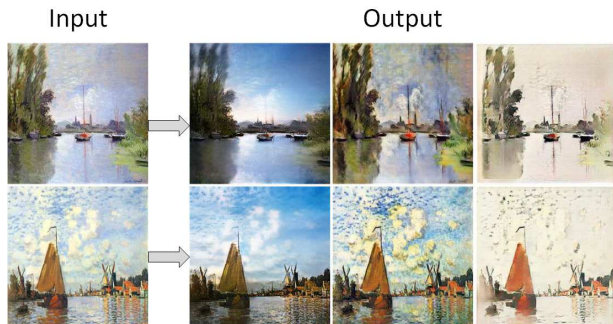


Figure 1: An example of image translation for MDT. It generates images in all domains regardless of the domain of the input image.

separate domains.

Despite many unsupervised methods [14] [15] [16] [17] [18] have succeeded in handling cross-domain image generation, they mainly consider the special case of one-to-one mapping. If the number of target transformation domains, denoted as  $N$ , is more than two, only single domain pairs can be used at a time during their training stage, resulting in  $N(N - 1)$  times of mutual training effort to meet the final requirements. With the increment of domains, simultaneous transformations for all domains become extremely complicated because separate training is inefficient and ineffective. A recent work called StarGAN [20] simplifies this issue by using only one mask vector and an encoder-decoder structure in generator. It is shown effective on transferring face attributes (e.g., hair color, expression, age, gender), but is not satisfactory enough at dealing with other domain styles. Another study named Domain-Bank [21] employs separate  $N$  encoders and  $N$  decoders to transform between any pair of domains. However, this method still has a complicated structure, and also one has to know the domains of input samples prior to testing, so that appropriate encoders can be specified.

In this paper, we present an unsupervised learning framework called multi-domain translator (MDT), extended from bi-directional image translation [14] [15] [17] to facilitate general style transformations for any number of domains. MDT has only one domain-

shared encoder for latent space embedding, and meanwhile adopts many identical domain-specified decoders. Such a design is to reduce model parameters and training cost compared to previous methods [21] [22]. During generation, our MDT does not need the source domain labels and is able to output results in all domains simultaneously, namely conduct “one-to-many” transformations. A multi-domain translation example is shown in Figure 1.

In order to improve the visual quality of transformed images, two constraints namely reconstruction loss and identity consistency loss are appended in the training stage. The former requires that when the model generates images in all domains, the generated domain-specified images (except the result in the source domain) could be recovered to their original appearance by feeding them to another cycled transformation. The latter enforces the generated images to remain unchanged when they are output by the decoders corresponding to their source domains. Mathematically, the reconstruction constraint is defined as  $G_i(G_j(x_i)) = x_i, i \neq j$ , while the identity consistency constraint is defined as  $G_i(x_i) = x_i$ , where  $x_i$  is the input image from domain  $i$  and  $G_i$  is the translator to transform images from any domain into domain  $i$ .

To validate the effectiveness of MDT, we apply it to several kinds of multi-domain image translation tasks with various number of domains and achieve high quality results. In addition, we adapt it to the two-domain situation and compare the results with several state-of-the-art methods [14] [15] that are successful in bi-directional image translation. Qualitative and quantitative comparative results demonstrate that MDT performs favorably against existing methods, demonstrating that the proposed framework offers a potential solution for general multi-domain image translation applications.

Our main contributions are three-fold:

- We propose Multi-Domain Translator (MDT), an efficient framework extended from bi-directional image translation to reduce the training effort. It performs both efficient and effective transformations for any given number of domains, achieving high generation quality.

- We introduce two multi-domain constraints called reconstruction loss and identity consistency loss, to further enhance the performance and visual quality of generation.
- We validate MDT on different databases and compare to representative state-of-the-art methods. All qualitative and quantitative evidences demonstrate that MDT performs favorably against them.

The reminder of the paper is organized as follows. Section 2 describes related work on image translation. Section 3 describes the proposed MDT in details. Experimental results, performance evaluation and comparisons are included in Section 4. Finally, conclusions are drawn in Section 5.

## 2 RELATED WORK

Benefiting from the development of GANs [19] family, many image generation problems have been obtained impressive results. Isola et al. introduce an image-to-image translation framework based on conditional GAN [13], which has been widely known as Pix2Pix [1]. They use paired images from two different domains and make one of them as a label to train. Their good performance on different cross-domain generation tasks has received an increasing amount of attention to the use of neural generative models [13] [23] [24] to study image translation problems.

### 2.1 Image-to-Image Translation

GANs are widely used in solving image translation problems. However, the original model [19] is trained through unsupervised learning that maps random noise to target image domain, which makes the generated images unpredictable. To control the content of the synthetic image, the improved supervised approaches train their networks with paired data [1] [13] to generate desired and high-precision target domain images. Although these supervised methods can transfer images between different domains, they still face the difficulty of collecting the corresponding labeled data to train. Therefore, unsupervised image

translation methods are favored by many researches who aim at achieving the same even better results as the supervised methods. An effective practice is usually to utilize two generators to cooperate with each other to constraint and complete the entire image generation [14] [17] [15]. Recent works, such as DiscoGAN [17], CycleGAN [14] and DualGAN [15], based on the same idea of cycle consistency to improve the quality of the generated images. The cycle consistency is an important constraint that requires the original image can be restored after successive two mappings by two different generators. On the other hand, Liu and Tuzel [25] propose CoGAN with tied weights on the first few layers for shared latent representation. Based on the idea of style transfer [3], Liu et al. propose a method UNIT [16] which exploits the content loss and the style loss between two domains to meet the requirements of image translation.

### 2.2 Multi-Domain Image Translation

Traditional image translation models only handle a mapping between two domains at a time. As the number of domains increases, the number of required models will exponential increase, actually  $O(N^2)$ . This makes them difficult to process the multi-domain image translation problems. Anoosheh et al. [22] who focus on reducing the complexity  $O(N^2)$  to  $O(N)$ , divide the generators into  $N$  encoders and  $N$  decoders, and combine them to any pair to complete the transformation between any two domains, called ComboGAN. A similarity idea can be found in Domain-Bank proposed by Hui et al. [21]. They adopt a weight sharing constraint in the last few layers of encoders and the first few layers of decoders, and an additional shared layers for the discriminators is also used to tied weights before the final output. Unlike the partition of generator, Choi et al. [20] use an auxiliary mask vector to label different domains and uses only one generator to translate multiple facial attributes, namely StarGAN. Huang et al. [26] directly extend UNIT [16] to multi-domain scenarios called MUNIT, which encodes the images from different domains to a shared content space and a domain-specific style space to solve both multi-domain and multi-modal image translation problems.

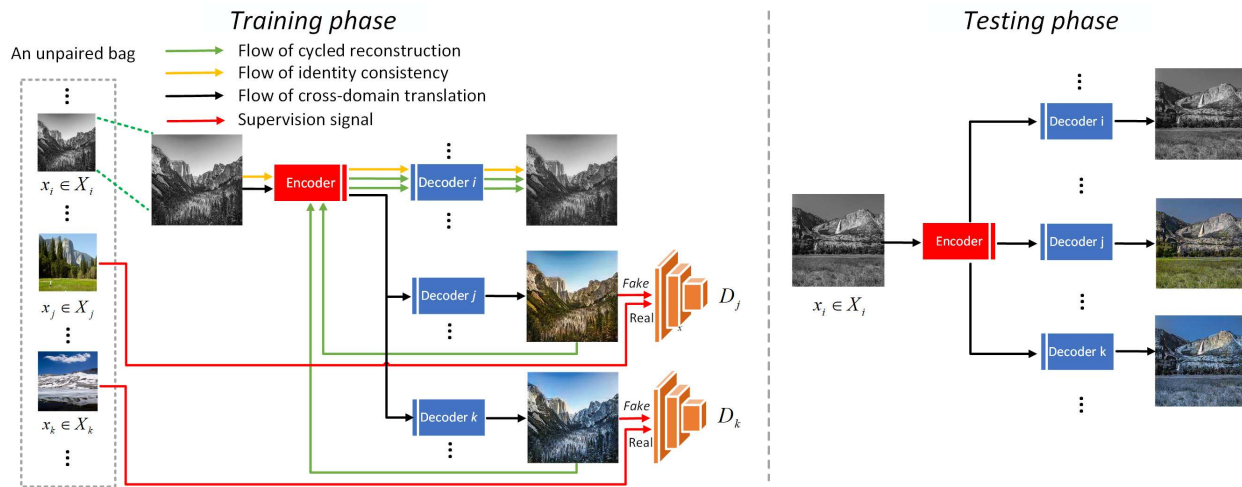


Figure 2: The main process of training and testing in each domain for our method. For an input image of each domain, all decoders will participate in the generation and output  $N$  fakes which will be also used to implement the two constraints and the discrimination during training.

All of aforementioned methods have good experimental results in their respective perspectives, but any of them still has typical deficiencies. For example, comboGAN [22] and Domain-Bank [21] have too many sub-models in their generator (nearly  $2N$ ) that need to be combined in pairs, and starGAN [20] is only effective in collections with small inter-domain differences due to the simple structure of its generator, while MUNIT [26] is based on the framework of style transfer [3] which needs other well-trained models [27] to assist, making training process inconvenient.

For our MDT, we make full use of a shared encoder and  $N$  identical domain decoders to output images in all domains, further reducing the training complexity, saving the cost of resources and making it unnecessary to judge the location of input domain during testing (Figure 4). In addition, we introduce a reconstruction consistency and an identity consistency to improve the quality of image generation.

### 3 PROPOSED METHOD

Given different domains represented by  $\mathbf{X}_i, i \in [1, N]$ , the task of multi-domain translation aims to find a representative mapping set  $\{F_{ij} : \mathbf{X}_i \rightarrow \mathbf{X}_j\}, i, j \in [1, N]$ . In order to simplify such  $O(N^2)$  complexity of mapping set, we in turn focus on functions  $\{F_i : \mathbf{X} \rightarrow \mathbf{X}_i\}$  that can map any source domains to a target domain, thus reducing the complexity to  $O(N)$  due to the regardless of any combination between input  $i$  and output  $j$ . Figure 3 illustrates the comparison of traditional solutions and our improved scheme in multi-domain translation.

For  $i \in [1, N]$ , we utilize a shared encoder  $E$  that encodes any single input  $x_i \in \mathbf{X}_i$  to a shared latent space, and provide a corresponding decoder  $G_j$  to map  $E(x_i)$  to any desired domain  $j$ . Here we use  $\hat{x}_{ij}$  to represent the output  $G_j(E(x_i))$ , which means an image from domain  $i$  transformed into domain  $j$ . Since there is only one encoder in our method, we rewrite  $G_j(E(x_i))$  to  $G_j(x_i)$  for the convenience of the following description.

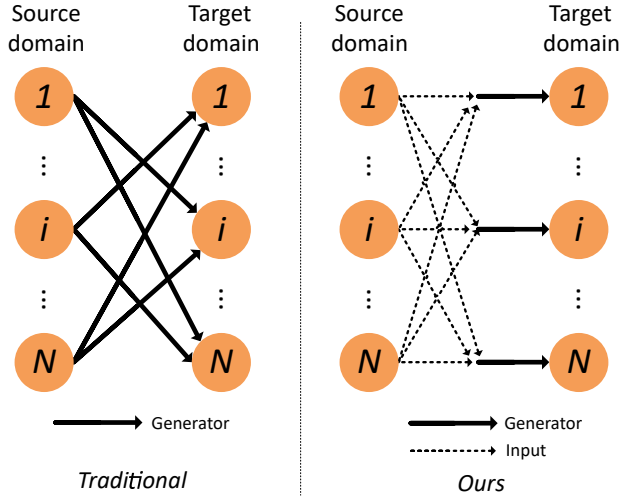


Figure 3: Image translation with multiple domains. For traditional methods, one generator only processes a domain pair, leading impossibility to meet the problem with large number domains. In our framework, the generator can map images from any domain to a target domain.

### 3.1 Objective

The overall objective can be described as below, which consists of three parts:

$$\mathcal{L} = \mathcal{L}_{GAN} + \lambda_{rec}\mathcal{L}_{rec} + \lambda_{idt}\mathcal{L}_{idt} \quad (1)$$

where  $\mathcal{L}_{GAN}, \mathcal{L}_{rec}, \mathcal{L}_{idt}$  represent the adversarial loss for GAN [19], the reconstruction loss and the identity loss for two constraints with their corresponding weights  $\lambda_{rec}$  and  $\lambda_{idt}$  to control their effects in training.

Here below, details of  $\mathcal{L}_{GAN}, \mathcal{L}_{rec}, \mathcal{L}_{idt}$  are described:

**Adversarial loss.** In unsupervised image-to-image translation, there are two mapping functions  $F_{ij} : \mathbf{X}_i \rightarrow \mathbf{X}_j, i, j \in \{1, 2\}, i \neq j$ , and the adversarial loss [19] can be described as:

$$\begin{aligned} \mathcal{L}_{ij}(G_j, D_j, \mathbf{X}_i, \mathbf{X}_j) &= \mathbb{E}_{x_j \sim P_{\mathbf{X}_j}} [f_1(D_j(x_j))] \\ &+ \mathbb{E}_{x_i \sim P_{\mathbf{X}_i}} [f_2(D_j(G_j(x_i)))] \quad (2) \end{aligned}$$

where  $D_j, G_j, P_{\mathbf{X}_i}$  respectively represent the discriminator and generator for domain  $j$  and the data distribution of  $\mathbf{X}_i$ , while the  $f_1, f_2$  functions can be specified as  $f_1(D) = \log(D), f_2(D) = \log(1 - D)$  or other forms in different models [1] [14] [28]. Following this objective, in MDT we extend it to the multi-domain scenario as:

$$\mathcal{L}_{GAN} = \sum_{i=1}^N \sum_{j=1}^N \mathcal{L}_{ij}, i \neq j \quad (3)$$

**Reconstruction loss.** Referred in the studies [14] [15] [17], reconstruction means that the input image should remain unchanged when it is successively processed by two generators with opposite input and output. This is an important idea which helps to constraint the generation so that the transformed image can retain more original contents and have the style of the target domain. If there are two domains  $\mathbf{X}_1, \mathbf{X}_2$  and two mapping functions  $G_1 : \mathbf{X}_2 \rightarrow \mathbf{X}_1, G_2 : \mathbf{X}_1 \rightarrow \mathbf{X}_2$ , the reconstruction requires  $G_1(G_2(\mathbf{X}_1)) = \mathbf{X}_1, G_2(G_1(\mathbf{X}_2)) = \mathbf{X}_2$ . To measure the the degree of approximation between  $G_1(G_2(\mathbf{X}_1))$  and  $\mathbf{X}_1, G_2(G_1(\mathbf{X}_2))$  and  $\mathbf{X}_2$ , we use the  $L_1$  distance as the metric because of the less blurring for generating images. So the reconstruction loss for  $\mathbf{X}_1, \mathbf{X}_2$  are  $\|G_1(G_2(\mathbf{X}_1)) - \mathbf{X}_1\|_1, \|G_2(G_1(\mathbf{X}_2)) - \mathbf{X}_2\|_1$ .

We generalize the reconstruction loss above to multi-domains for MDT. The underlying intuition is that an input image from domain  $i$  can be restore again after being transformed into all other domains except its source domain. Since an input image will be transformed into  $N - 1$  domains except its own domain, there are  $N - 1$  reconstruction terms by feeding each generated domain image ( $G_j(x_i)$ ) to its own generator  $G_i$ . Thus, the reconstruction loss for any input data  $i$  can be defined as:

$$\mathcal{L}_i^{rec} = \sum_{j=1}^N \|G_i(G_j(x_i)) - x_i\|_1, j \neq i \quad (4)$$

For the total loss of reconstruction, we only need to add up all the losses of each input domain:

$$\mathcal{L}_{rec} = \sum_{i=1}^N \mathcal{L}_i^{rec} \quad (5)$$

**Identity loss.** In addition to reconstruction loss, we also introduce another loss as an extra constraint for generation where we followed the idea of CycleGAN [14] and extend it to multiple domains. The key is that when a domain generator processes an image from its own domain, it should allow the image to pass through without any changes. Thus the identity constraint means the invariance of generation in the generator’s own domain, which helps to enforce the generator to learn its domain features. We use the same metric as the reconstruction loss to preserve the identity of  $i$ , namely:

$$\mathcal{L}_i^{idt} = \|G_i(x_i) - x_i\|_1 \quad (6)$$

The total identity loss is thus defined as:

$$\mathcal{L}_{idt} = \sum_{i=1}^N \mathcal{L}_i^{idt} \quad (7)$$

Regarding to the two constraints  $\mathcal{L}_{idt}$  and  $\mathcal{L}_{rec}$ , we can use a matrix equation to express them. As shown below, the column vector is a representative of the input data for all domains, and row vector contains all domain generators, while  $\hat{x}_{ij}$  represents that the image from domain  $i$  has been converted to domain  $j$  by the generator  $G_j$ . Therefore, the diagonal elements of the output matrix are always used to perform identity loss and the rest are used for reconstruction constraint.

$$\begin{pmatrix} x_1 \\ \vdots \\ x_i \\ \vdots \\ x_N \end{pmatrix} (G_1 \cdots G_i \cdots G_N) = \begin{pmatrix} \hat{x}_{11} & \cdots & \hat{x}_{1i} & \cdots & \hat{x}_{1N} \\ \vdots & \ddots & \vdots & \ddots & \vdots \\ \hat{x}_{i1} & \cdots & \hat{x}_{ii} & \cdots & \hat{x}_{iN} \\ \vdots & \ddots & \vdots & \ddots & \vdots \\ \hat{x}_{N1} & \cdots & \hat{x}_{Ni} & \cdots & \hat{x}_{NN} \end{pmatrix} \quad (8)$$

### 3.2 Architecture

To implement the functions  $F_i : \mathbf{X} \rightarrow \mathbf{X}_i$ , we only use one shared encoder that handles images re-

gardless of their domain, and  $N$  identical encoders matched with a corresponding discriminator to generate the transformed results in all domains. Here we apply a U-net [23] structure in generator, where in decoding stage, the features deconvoluted by each up-sampling layers are connected with the same size features convoluted by down-sampling layers, and then they are deconvoluted again until the final output. At the tail of the encoder and the head of decoder, we add several residual blocks [29] to enhance the generation in multi-domain case. For the discriminator, We additionally use Markovian patchGAN [30] architecture to discriminate local information, which means there are two outputs in a discriminator, an array and a scalar for the discrimination of local and entire image respectively. We assign a discriminator to each domain and train the discriminator with real and fake images from the corresponding domain. Figure 4 illustrates the detailed architecture of these networks.

### 3.3 Algorithm

Even if we ignore the consideration of input domain, it seems that we should train  $N$  GAN models separately. Actually, the difference is that we treat all decoders as a whole and need to accumulate all the losses from different domains and then use a gradient descent method to update the parameters. Figure 2 demonstrates the procedure of training and testing stage. In a training epoch, each domain is processed at least once with using the corresponding discriminator and two constraints under all domains. For the test, we only need to provide an image from any domain to the generator, and then we will get the transformed results of all domains. To detail the training procedure, we list the pseudo code for all steps without considering the specific implementation or any algorithm used in each step, as shown in Algorithm 1.

## 4 EXPERIMENTS

In order to access the performance of MDT in multi-domain image translation, we conduct experiments

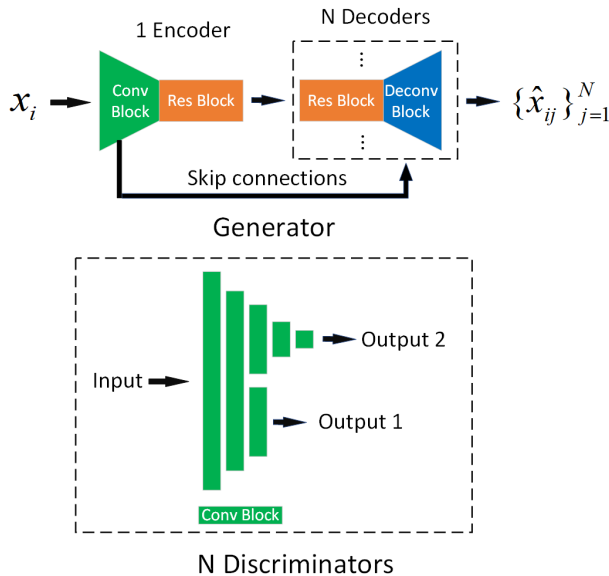


Figure 4: The architecture of our generator and discriminator. The generator has one encoder and  $N$  identical decoders, and outputs  $N$  fake images. For discriminator, there are two outputs used for the judgment of local and entire image.

with a number of domains on different databases including cross-databases. In the evaluation of bi-directional and multi-domain image translation tasks, we compare MDT against the state-of-the-art methods in two-domain image translation. The results demonstrate that using MDT to process multi-domain image translation tasks is superior not only in performance but also in time-consuming than using the bi-directional translators. Lastly, we investigate the effectiveness of various components of the two constraints.

#### 4.1 Training Details

In all experiments, we set same super parameters and implement our method by PyTorch [31] with the aid of a NVIDIA RTX 2080 Ti X GPU. For the images, we resize them to  $256 \times 256$ , and make sure that there

**Algorithm 1** MDT training procedure.  $N$  is the number of domains and  $x_i$  is a sample in its corresponding domain  $\mathbf{X}_i$ , while  $\hat{x}_{ij} = G_j(x_i)$  represents the transformed result in domain  $j$  with the input domain data  $x_i$ .

- 1: **for** number of training iterations **do**
- 2:   Initialize the loss to zero for both discriminators and generator.
- 3:   Randomly get sample images  $\{x_i\}_{i=1}^N$ .
- 4:   Use  $\{x_i\}_{i=1}^N$  to generate fake images  $\{\hat{x}_{ij}\}_{i,j=1}^N$ .
- 5:   Use  $\{x_i\}_{i=1}^N$  as the real labels to compute the loss of discriminators.
- 6:   Use  $\{\hat{x}_{ij}\}_{i,j=1}^N, i \neq j$  as the fake labels to compute the loss of discriminators.
- 7:   For discriminators, use their loss to update their parameters.
- 8:   Use  $\{\hat{x}_{ij}\}_{i,j=1}^N, i = j$  to compute  $\mathcal{L}_{idt}$ .
- 9:   Use  $\{\hat{x}_{ij}\}_{i,j=1}^N, i \neq j$  to compute  $\mathcal{L}_{rec}, \mathcal{L}_{GAN}$ .
- 10:   Get the total loss of generator  $\mathcal{L} = \mathcal{L}_{GAN} + \lambda_{rec}\mathcal{L}_{rec} + \lambda_{idt}\mathcal{L}_{idt}$ .
- 11:   Use the loss  $\mathcal{L}$  to update the parameters of generator.
- 12: **end for**

is no overlap between the training set and testing set.

For training, we use the Adam optimizer [32] with momentum parameters  $\beta_1 = 0.5$ ,  $\beta_2 = 0.999$  and a batch size of 1. The leaky rectified linear units (leakyReLU) with a slope of 0.2 is selected as the non linearity activation after instance normalization [33]. All models are trained from scratch with a variable learning rate which is a constant value 0.0002 in the first half of epochs and then is linearly decayed to zero over the rest epochs. We only iterate the training process 50 epochs because the quality of generated images at this time is good enough.

For the encoder and decoders in our generator, we use convolutional and de-convolutional filters with size-4, stride-2 and padding-1 to down- and up-sampling, and respectively attach 6 residual blocks [29] to the end of convolution and the beginning of de-convolution. For the discriminators, we use the entire image to classify whether it is real or fake,



and also adopt  $70 \times 70$  PatchGANs [30] to judge the overlapping image patches which is recommended by Pix2Pix [1]. These two networks are tied with weights by three shared convolutional layers and are combined together in one discriminator to output two judgments. For the weights of reconstruction loss and identity loss, we set  $\lambda_{rec} = \lambda_{idt} = 10$ .

## 4.2 Qualitative Results

We show several examples achieved on different database and different number of domains.

Figure 5 shows an example of image translation task among summer, winter and black-white photographs. The BW images are randomly selected from the two seasons and are converted to grayscale photos. In Figure 7, we transfer scenic photos and 4 different artistic painting styles into each other. It is obvious that MDT has good visual effects in style transfer. The two databases are download directly from the website of CycleGAN [14], where each domain includes hundreds or thousands of images for training, as well as tens or hundreds for testing. All of them are collected respectively from Flickr and ImageNet [34].

In addition to test in same database, we conduct cross-dataset validation with using various databases for experimentation, where we aim at face synthesis between photos and sketches from three databases. These databases are the Chinese University of Hong Kong (CUHK) face sketch database (CUFS) [35], the CUHK Face Sketch FERET [36] Database (CUFSF) [37] and the IIIT-D Viewed Sketch Database (IIIT-D) [38], all of which have hundreds of face photo-sketch image pairs. We only choose the face photos from CUFS and the other three different styles of face sketches from these three databases. So this task contains 4 different domains to mutual translation. Figure 6 shows the experimental results where we are clear to see the good performance of MDT in face synthesis.

For more domains to transform, we use the MultiPIE database [39] which is a large dataset for face recognition including more than 750, 000 images under 15 poses, 20 illuminations and 6 expressions, taken from 337 subjects of different ages, genders,

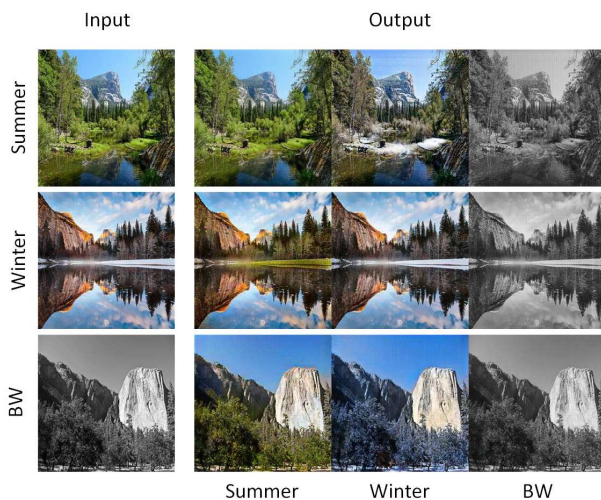


Figure 5: Example of image translation among summer, winter and BW photos. The left column contains the input from different domains and the right three columns represent the output in different domains. Each row represents the input and all transformed results.

faces and whether they wear glasses or not. The task is face re-lighting among 8 different illuminations with same pose and expression. The face images are selected from 249 subjects and are cropped by the face detector S<sup>3</sup>FD [40] without strict alignment. In each lighting domain, We divide the 249 images into 150 for training and 99 for testing. A part of transformed images are shown in Figure 8, where we are clear to see that the quality of transformed image dose not degrade with the increasing number of domains although there is only one encoder in our generator.

## 4.3 Comparison And Evaluation

In this section, we compare MDT with the state-of-the-art methods, and show the advantages of MDT not only in bi-directional image translation but also in multiple-domain scenario.



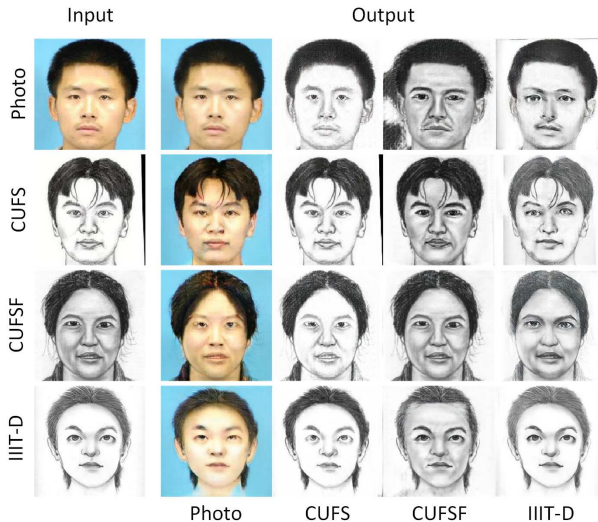


Figure 6: Example of face synthesis among face photos and face sketches in different styles. Face photos are from the CUFS database, and face sketches are from CUFS ,CUFSF, IIIT-D respectively.

#### 4.3.1 Bidirectional image translation

Although MDT is to reduce the complexity in multiple domains, it has good performance in bi-directional image translation tasks. We use two kinds of paired and unpaired data to conduct experiments separately, and compare with CycleGAN [14] and DualGAN [15] which are the stat-of-the-art methods in two-domain image translation and can process high resolution of  $256 \times 256$ . For CycleGAN, we use pre-trained models downloaded from the author’s website to test. For DualGAN, we train it with the default parameters recommended in the official code.

Figure 9 presents the results of using these three methods on unpaired dataset that is collected from ImageNet [34] by zhu et.al [14]. Compared to these two stat-of-the-art methods, our approach transforms the images more realistically and accurately without obvious artifacts and contamination of non-target objects.

Training with paired data seems to be supervised

learning because the input for each generator corresponds to each other. Here we utilize CMP Facades [41] which includes architectural labels and photos for semantic segmentation. As shown in Figure 10, our translated results are visually comparable to the two methods on the task of label to photo, but are slightly weaker than CycleGAN on the photo to label task. In fact, the performance of MDT in supervised learning is a little inferior to that in unsupervised learning.

#### 4.3.2 Multi-domain image translation

To further demonstrate the advantages of our approach in image translation, we compare bi-directional translators with MDT in an experiment with the least number of domains in multi-domain translation. We exploit the face re-lighting task stated in 4.2 because the illuminations of each subject in this database [39] can be respectively regarded as ground truth so that we can reference them to quantify the transformed results. Detailedly, We choose 3 illuminations with significant differences in dark, normal and shadow from each subject to represent the different domains. So this task contains 6 cases of bi-directional translations. We use two one-to-one mapping methods, CycleGAN [14] and DualGAN [15] to complete this task, and compare the results with our MDT shown in Figure 11.

As far as face synthesis, face recognition rate is often used as an evaluation metric. However, we can not make a meaningful comparison with using this measurement due to the 100% accuracy in all transformed results computed by deep feature extractors [29] [42] which have been trained with large scale database [43] and have strong robustness to the variation of illumination. Therefore, we focus on full reference image quality assessment (FR-IQA), and utilize two metrics of feature similarity index (FSIM) [44] and structural similarity index (SSIM) [45] to respectively evaluate the quality of images generated by of these methods. The two metrics are used to measure the similarity between two images. If two images are similar, both the FSIM and SSIM values are close to 1, which represents the quality of generated images referenced to ground truth. Table 2 shows the mean

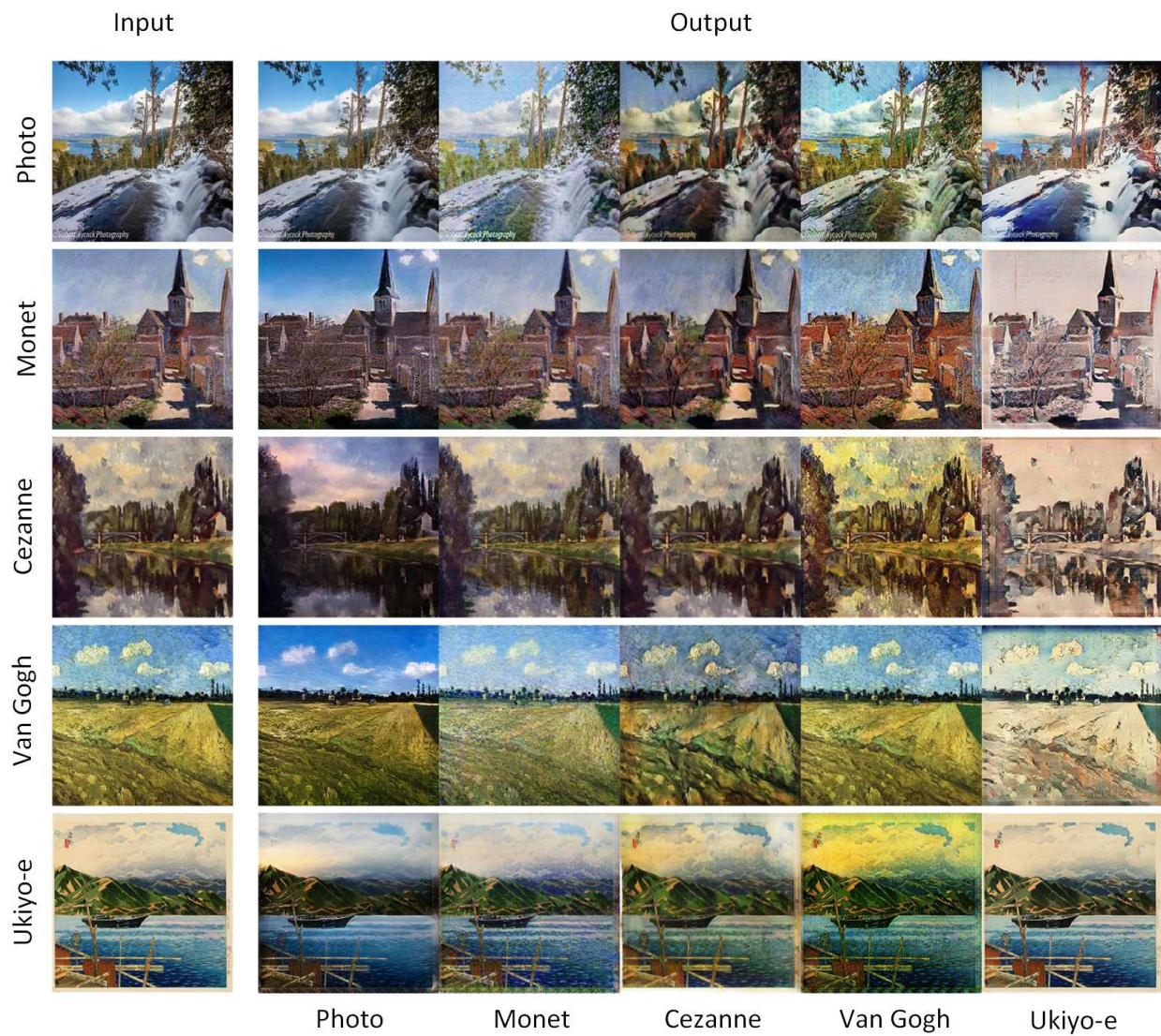


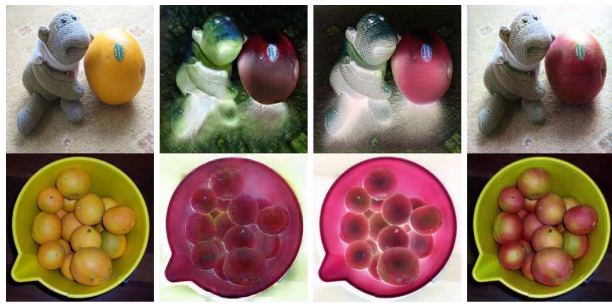
Figure 7: Example of style transfer among photographic, Monet, Cezanne, Van Gogh and Ukiyo-e.





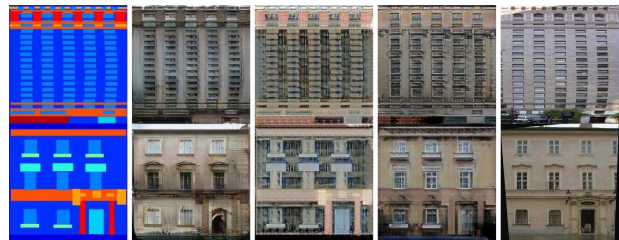


Input      CycleGAN      DualGAN      MDT  
 (a) apple  $\rightarrow$  orange

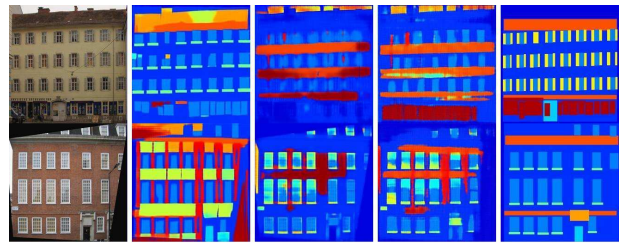


Input      CycleGAN      DualGAN      MDT  
 (b) orange  $\rightarrow$  apple

Figure 9: Results of different methods on the task of apple  $\leftrightarrow$  photo.



Input      CycleGAN      DualGAN      MDT      GT  
 (a) semantic label  $\rightarrow$  photo



Input      CycleGAN      DualGAN      MDT      GT  
 (b) photo  $\rightarrow$  semantic label

Figure 10: Results of different methods on the task of semantic label  $\leftrightarrow$  photo.

Table 1: Total cost of training time and parameters using different methods in the three-domain face re-lighting task. For a two-domain translator, the cost is the sum of consumption in all 6 cases.

Method	Cost	Time	Parameters
	CycleGAN		8.1h
DualGAN		2.1h	342M
MDT		<b>1.6h</b>	155M

values and standard deviations of FSIM and SSIM for the 6 cases and the overall task. Both the measurements demonstrate the superiority of MDT in most cases. For more details of the overall assessment, we present the evaluation curves to illustrate the quality distribution of the generated images. As shown in Figure 12, the vertical axis indicates the percentage of images whose FR-IQA values are higher than the values on the horizontal axis. Our method almost has higher percentage on all IQA-values.

Furthermore, Table 1 shows the training time for convergence and the total number of parameters under different methods on this task. MDT saves more time in training, however, it has more parameters than CycleGAN. This is because CycleGAN has a variety of network structures in generator, when it has the same structure of U-net [23], it will have more parameters than us. As the number of domains increases, the resource consumption will increase exponentially for these two methods, but it will increase linearly for MDT. Actually, the parameters of MDT are increased approximately according to the formula:

$$Params \approx 1.14 \times 10^8 + 4.1 \times 10^7 \times (N - 2) \quad (9)$$

Thus, when there are a large number of domains in image translation, the advantage of CycleGAN in parameter numbers will be gone.

In sum, all the results demonstrate that MDT performs favorably against the bi-directional image translators in both image generation and training cost.



Figure 11: Different methods for face re-lighting among 3 different illuminations of normal, shadow and dark. From left to right: input, CycleGAN [14], DualGAN [15], MDT (ours) and ground truth.



Table 2: The mean values and standard deviations using different methods on the three-domain face re-lighting task, including 6 cases of bi-directional translation in total, evaluated by the metrics of FSIM and SSIM.

Metric \ Method \ Task	FSIM			SSIM		
	CycleGAN	DualGAN	MDT	CycleGAN	DualGAN	MDT
normal → shadow	0.906±0.018	0.902±0.015	<b>0.916±0.016</b>	0.883±0.043	0.865±0.028	<b>0.898±0.040</b>
normal → dark	<b>0.939±0.013</b>	0.925±0.013	0.935±0.012	<b>0.938±0.030</b>	0.928±0.017	0.934±0.031
shadow → normal	0.883±0.017	0.882±0.017	<b>0.894±0.019</b>	0.858±0.059	0.855±0.049	<b>0.872±0.056</b>
shadow → dark	0.951±0.011	0.946±0.009	<b>0.955±0.011</b>	0.951±0.018	0.948±0.011	<b>0.954±0.025</b>
dark → normal	<b>0.889±0.020</b>	0.885±0.016	0.887±0.019	<b>0.860±0.060</b>	0.852±0.054	0.858±0.065
dark → shadow	0.924±0.016	0.925±0.014	<b>0.933±0.011</b>	0.906±0.044	0.905±0.048	<b>0.910±0.044</b>
Overall	0.915±0.030	0.911±0.027	<b>0.920±0.028</b>	0.900±0.057	0.892±0.054	<b>0.904±0.056</b>

#### 4.4 Ablation Study

In order to investigate the effectiveness of the two constraints in the proposed method, we isolate the items of reconstruction, identity and adversarial loss, and respectively train the network to perform the three-domain face re-lighting task stated in 4.3.2.

Figure 13 shows an example of mapping the lighting from dark to normal and shadow under 4 different components in training. It is obvious that the image quality is improved with using reconstruction and identity constraints. To be objective, we respectively compute the overall results of mean values and standard deviations by the metrics of FSIM [44] and SSIM [45] shown in Table 3 where indicates the effectiveness of adding the reconstruction and identity loss in training. More details are draw in Figure 14. Without either of these two constraints, the results are substantially degrade.

In particular, compared to the identity loss, the reconstruction loss is more conducive to improve generation, possibly because it has more processing and learning objectives than the other. In identity constraint, the decoder only focuses on learning the feature of its own domain through one input image, but in reconstruction constraint, it needs to use the learned domain features to restore  $N - 1$  fake images.

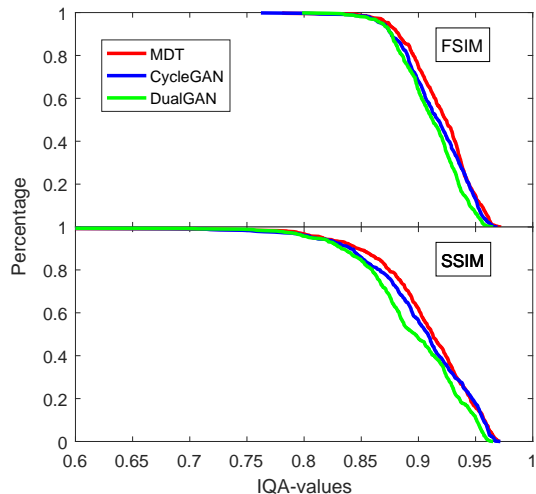


Figure 12: FR-IQA values of all images generated in the entire task using different methods on the three-domain translation. Top and bottom: FSIM and SSIM values.



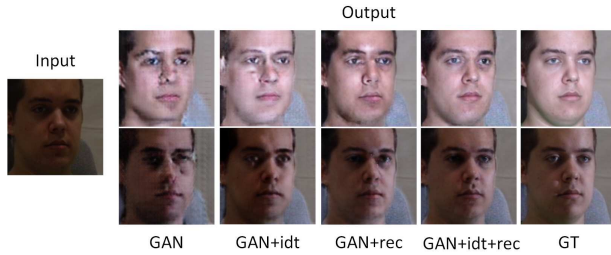


Figure 13: Different variants of our method for the transformation among three face illuminations. We only show an example of mapping the dark lighting to normal and shadow lighting. From left to right: input, adversarial loss alone, GAN with identity loss, GAN with reconstruction loss, our full loss and ground truth.

## 5 CONCLUSIONS

We propose a novel unsupervised method for multi-domain image translation called Multiple Domain Translator (MDT), whose generator contains a shared encoder and  $N$  identical decoders for each domain. Using MDT, the training complexity is reduced from  $O(N^2)$  to  $O(N)$ , which saves the cost of time and calculating space and makes it easy to process image translation problems among any number of domains. To enhance the generation, we further introduce two constraints of reconstruction and identity extended from bi-directional image translation, both of which can significantly improve the quality of synthetic image. In both of qualitative and quantitative evaluations of image translation tasks under two or more domains, MDT is superior to the state-of-the-art bi-directional translators [15] [14]. In future work, we would like to extend MDT to handle other mixed domains, such as text, video or even audio.

## ACKNOWLEDGMENT

This work was supported by the Joint Funds of the National Natural Science Foundation of China under Grant U1833128, and was partly supported by

Table 3: The mean values and standard deviations on the three-domain face re-lighting task using different loss in training, evaluated by the metrics of FSIM and SSIM.

Loss	Metric	FSIM	SSIM
	GAN		0.868±0.031
GAN+idt		0.893±0.032	0.841±0.068
GAN+rec		0.909±0.031	0.878±0.070
GAN+rec+idt		<b>0.920±0.028</b>	<b>0.904±0.056</b>

the National Science Foundation of China, under No. 61703077, the Fundamental Research Funds for the Central Universities No. YJ201755, and the Sichuan Science and Technology Major Projects (2018GZDZX0029).

## References

- [1] P. Isola, J.-Y. Zhu, T. Zhou, A. A. Efros, Image-to-image translation with conditional adversarial networks, in: 2017 IEEE Conference on Computer Vision and Pattern Recognition (CVPR), 2017, pp. 5967–5976.
- [2] G. Papandreou, L.-C. Chen, K. P. Murphy, A. L. Yuille, Weakly-and semi-supervised learning of a deep convolutional network for semantic image segmentation, in: 2015 IEEE International Conference on Computer Vision (ICCV), 2015, pp. 1742–1750.
- [3] J. Johnson, A. Alahi, L. Fei-Fei, Perceptual losses for real-time style transfer and super-resolution, in: European Conference on Computer Vision (ECCV), 2016, pp. 694–711.
- [4] R. Zhang, P. Isola, A. A. Efros, Colorful image colorization, in: European Conference on Computer Vision, 2016, pp. 649–666.
- [5] B. Abboud, F. Davoine, M. Dang, H. Laboratory, Expressive face recognition and synthesis, Proceedings / CVPR, IEEE Computer So-

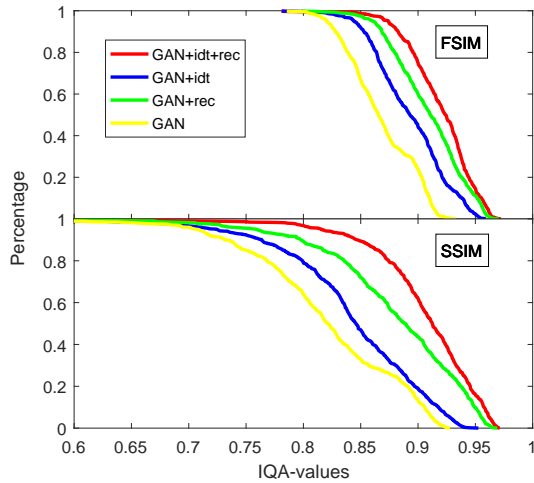


Figure 14: FR-IQA values of all generated images using various loss components in our method on the three-domain translation. Top and bottom: FSIM and SSIM values.

ciety Conference on Computer Vision and Pattern Recognition. IEEE Computer Society Conference on Computer Vision and Pattern Recognition.

- [6] H. Kazemi, M. Iranmanesh, A. Dabouei, S. Soleymani, N. M. Nasrabadi, Facial attributes guided deep sketch-to-photo synthesis, in: 2018 IEEE Winter Applications of Computer Vision Workshops (WACVW), 2018, pp. 1–8.
- [7] D. Pathak, P. Krhenbhl, J. Donahue, T. Darrell, A. A. Efros, Context encoders: Feature learning by inpainting, in: 2016 IEEE Conference on Computer Vision and Pattern Recognition (CVPR), 2016, pp. 2536–2544.
- [8] B. Xiao, J. Zhou, A. Robles-Kelly, Pattern recognition for high performance imaging, Pattern Recognition 82.
- [9] C. Ledig, L. Theis, F. Huszar, J. Caballero, A. Cunningham, A. Acosta, A. P. Aitken, A. Tejani, J. Totz, Z. Wang, W. Shi, Photo-realistic

single image super-resolution using a generative adversarial network, in: 2017 IEEE Conference on Computer Vision and Pattern Recognition (CVPR), 2017, pp. 105–114.

- [10] A. A. Efros, W. T. Freeman, Image quilting for texture synthesis and transfer, in: Proceedings of the 28th annual conference on Computer graphics and interactive techniques, 2001, pp. 341–346.
- [11] T. Chen, M.-M. Cheng, P. Tan, A. Shamir, S.-M. Hu, Sketch2photo: internet image montage, international conference on computer graphics and interactive techniques 28 (5) (2009) 124.
- [12] J. Long, E. Shelhamer, T. Darrell, Fully convolutional networks for semantic segmentation, in: 2015 IEEE Conference on Computer Vision and Pattern Recognition (CVPR), 2015, pp. 3431–3440.
- [13] M. Mirza, S. Osindero, Conditional generative adversarial nets, arXiv preprint arXiv:1411.1784.
- [14] J.-Y. Zhu, T. Park, P. Isola, A. A. Efros, Unpaired image-to-image translation using cycle-consistent adversarial networks, in: 2017 IEEE International Conference on Computer Vision (ICCV), 2017, pp. 2242–2251.
- [15] Z. Yi, H. Zhang, P. Tan, M. Gong, Dualgan: Unsupervised dual learning for image-to-image translation, in: 2017 IEEE International Conference on Computer Vision (ICCV), 2017, pp. 2868–2876.
- [16] M.-Y. Liu, T. Breuel, J. Kautz, Unsupervised image-to-image translation networks, in: Advances in Neural Information Processing Systems, 2017, pp. 700–708.
- [17] T. Kim, M. Cha, H. Kim, J. K. Lee, J. Kim, Learning to discover cross-domain relations with generative adversarial networks, in: ICML’17 Proceedings of the 34th International Conference on Machine Learning - Volume 70, 2017, pp. 1857–1865.

- [18] Y. Taigman, A. Polyak, L. Wolf, Unsupervised cross-domain image generation, in: ICLR 2017 : International Conference on Learning Representations 2017, 2017.
- [19] I. J. Goodfellow, J. Pouget-Abadie, M. Mirza, B. Xu, D. Warde-Farley, S. Ozair, A. C. Courville, Y. Bengio, Generative adversarial nets, in: Advances in Neural Information Processing Systems 27, 2014, pp. 2672–2680.
- [20] Y. Choi, M. Choi, M. Kim, J.-W. Ha, S. Kim, J. Choo, Stargan: Unified generative adversarial networks for multi-domain image-to-image translation, in: 2018 IEEE/CVF Conference on Computer Vision and Pattern Recognition, 2018, pp. 8789–8797.
- [21] L. Hui, X. Li, J. Chen, H. He, J. Yang, Unsupervised multi-domain image translation with domain-specific encoders/decoders, in: 2018 24th International Conference on Pattern Recognition (ICPR), 2018, pp. 2044–2049.
- [22] A. Anoosheh, E. Agustsson, R. Timofte, L. V. Gool, Combogan: Unrestrained scalability for image domain translation, in: 2018 IEEE/CVF Conference on Computer Vision and Pattern Recognition Workshops (CVPRW), 2018, pp. 783–790.
- [23] O. Ronneberger, P. Fischer, T. Brox, U-net: Convolutional networks for biomedical image segmentation, medical image computing and computer assisted intervention (2015) 234–241.
- [24] D. P. Kingma, M. Welling, Auto-encoding variational bayes, in: ICLR 2014 : International Conference on Learning Representations (ICLR) 2014, 2014.
- [25] M.-Y. Liu, O. Tuzel, Coupled generative adversarial networks, arXiv preprint arXiv:1606.07536.
- [26] X. Huang, M.-Y. Liu, S. J. Belongie, J. Kautz, Multimodal unsupervised image-to-image translation, in: Proceedings of the European Conference on Computer Vision (ECCV), 2018, pp. 179–196.
- [27] K. Simonyan, A. Zisserman, Very deep convolutional networks for large-scale image recognition, in: ICLR 2015 : International Conference on Learning Representations 2015, 2015.
- [28] I. Gulrajani, F. Ahmed, M. Arjovsky, V. Dumoulin, A. C. Courville, Improved training of wasserstein gans, in: Advances in Neural Information Processing Systems, 2017, pp. 5767–5777.
- [29] K. He, X. Zhang, S. Ren, J. Sun, Deep residual learning for image recognition, in: 2016 IEEE Conference on Computer Vision and Pattern Recognition (CVPR), 2016, pp. 770–778.
- [30] C. Li, M. Wand, Precomputed real-time texture synthesis with markovian generative adversarial networks, in: European Conference on Computer Vision, 2016, pp. 702–716.
- [31] B. Steiner, Z. DeVito, S. Chintala, S. Gross, A. Paszke, F. Massa, A. Lerer, G. Chanan, Z. Lin, E. Yang, A. Desmaison, A. Tejani, A. Kopf, J. Bradbury, L. Antiga, M. Raison, N. Gimelshein, S. Chilamkurthy, T. Killeen, L. Fang, J. Bai, Pytorch: An imperative style, high-performance deep learning library, in: NeurIPS 2019 : Thirty-third Conference on Neural Information Processing Systems, 2019.
- [32] D. P. Kingma, J. L. Ba, Adam: A method for stochastic optimization, international conference on learning representations.
- [33] D. Ulyanov, A. Vedaldi, V. S. Lempitsky, Instance normalization: The missing ingredient for fast stylization., arXiv preprint arXiv:1607.08022.
- [34] J. Deng, W. Dong, R. Socher, L.-J. Li, K. Li, L. Fei-Fei, Imagenet: A large-scale hierarchical image database, in: 2009 IEEE Conference on Computer Vision and Pattern Recognition, 2009, pp. 248–255.
- [35] X. Wang, X. Tang, Face photo-sketch synthesis and recognition, IEEE Transactions on Pattern

- Analysis and Machine Intelligence 31 (11) (2009) 1955–1967.
- [36] P. Phillips, H. Moon, S. Rizvi, P. Rauss, The feret evaluation methodology for face-recognition algorithms, *IEEE Transactions on Pattern Analysis and Machine Intelligence* 22 (10) (2000) 1090–1104.
- [37] W. Zhang, X. Wang, X. Tang, Coupled information-theoretic encoding for face photo-sketch recognition, in: *CVPR 2011*, 2011, pp. 513–520.
- [38] H. S. Bhatt, S. Bharadwaj, R. Singh, M. Vatsa, Memetic approach for matching sketches with digital face images.
- [39] R. Gross, I. Matthews, J. Cohn, T. Kanade, S. Baker, Multi-pie, *Image and Vision Computing* 28 (5) (2010) 807–813.
- [40] S. Zhang, X. Zhu, Z. Lei, H. Shi, X. Wang, S. Z. Li, S<sup>3</sup>fd: Single shot scale-invariant face detector, in: *2017 IEEE International Conference on Computer Vision (ICCV)*, 2017, pp. 192–201.
- [41] R. Š. Radim Tyleček, Spatial pattern templates for recognition of objects with regular structure, in: *Proc. GCPR*, Saarbrücken, Germany, 2013.
- [42] X. Wu, R. He, Z. Sun, T. Tan, A light cnn for deep face representation with noisy labels, *IEEE Transactions on Information Forensics and Security* 13 (11) (2018) 2884–2896.
- [43] Q. Cao, L. Shen, W. Xie, O. M. Parkhi, A. Zisserman, Vggface2: A dataset for recognising faces across pose and age, in: *2018 13th IEEE International Conference on Automatic Face and Gesture Recognition (FG 2018)*, 2018, pp. 67–74.
- [44] L. Zhang, L. Zhang, X. Mou, D. Zhang, Fsim: A feature similarity index for image quality assessment, *IEEE Transactions on Image Processing* 20 (8) (2011) 2378–2386.
- [45] Z. Wang, A. Bovik, H. Sheikh, E. Simoncelli, Image quality assessment: from error visibility to structural similarity, *IEEE Transactions on Image Processing* 13 (4) (2004) 600–612.